



저작자표시-비영리-변경금지 2.0 대한민국

이용자는 아래의 조건을 따르는 경우에 한하여 자유롭게

- 이 저작물을 복제, 배포, 전송, 전시, 공연 및 방송할 수 있습니다.

다음과 같은 조건을 따라야 합니다:



저작자표시. 귀하는 원저작자를 표시하여야 합니다.



비영리. 귀하는 이 저작물을 영리 목적으로 이용할 수 없습니다.



변경금지. 귀하는 이 저작물을 개작, 변형 또는 가공할 수 없습니다.

- 귀하는, 이 저작물의 재이용이나 배포의 경우, 이 저작물에 적용된 이용허락조건을 명확하게 나타내어야 합니다.
- 저작권자로부터 별도의 허가를 받으면 이러한 조건들은 적용되지 않습니다.

저작권법에 따른 이용자의 권리는 위의 내용에 의하여 영향을 받지 않습니다.

이것은 [이용허락규약\(Legal Code\)](#)을 이해하기 쉽게 요약한 것입니다.

[Disclaimer](#)

工學碩士 學位論文

**Thermal Characteristics of  
Ytterbium-doped Phosphosilicate  
Fiber Amplifiers**

Ytterbium-doped Phosphosilicate 광섬유 증  
폭기의 온도 의존성에 대한 연구

2012년 8월

서울대학교 대학원

전기 컴퓨터 공학부

Seung Jong Lee

# Thermal Characteristics of Ytterbium-doped Phosphosilicate Fiber Amplifiers

지도 교수 정 윤 찬

이 논문을 공학석사 학위논문으로 제출함  
2012 년 5 월

서울대학교 대학원  
전기 컴퓨터 공학부  
이 승 종

이승종의 공학석사 학위논문을 인준함  
2012 년 5 월

위 원 장 \_\_\_\_\_ (인)

부위원장 \_\_\_\_\_ (인)

위 원 \_\_\_\_\_ (인)

Abstract

# **Thermal Characteristics of Ytterbium-doped Phosphosilicate Fiber Amplifiers**

Seung Jong Lee

Department of Electrical Engineering and Computer Science  
College of Engineering  
Seoul National University

Among rare-earth-doped fibers, ytterbium-doped (Yb) silica fibers exhibit absolutely outstanding performances especially in the high power regime where nonlinearity and thermal control of the system is crucial. In order to achieve higher power with fiber lasers and amplifiers, higher rare-earth doping level is required. However, high level of rare-earth concentration in limited core size and fiber length can cause clustering, reduced lifetime, and photo-darkening.

Phosphosilicate-based ytterbium-doped fibers demonstrate substantially longer lifetime and negligible photo-darkening compared to aluminosilicate-based fibers and higher damage threshold than the phosphate glass fibers. Ytterbium-doped phosphosilicate fiber is a viable option for high power lasers and amplifiers. Although there have been a number of studies on thermal characteristics of ytterbium-doped fibers, most reports are for aluminosilicate-based ytterbium-doped fibers so that information about thermal characteristics of ytterbium-doped phosphosilicate fiber is very limited to date.

In this thesis, thermal characteristics of an ytterbium-doped phosphosilicate fiber, including the temperature-dependent absorption and emission cross-sections and the fluorescence lifetime are presented. A tunable cladding-pumped fiber laser amplifier based on the ytterbium-doped phosphosilicate fiber is characterized with changing temperature to investigate

their influence on the gain. Study presented here should improve the accuracy of modeling Ytterbium-doped phosphosilicate fiber lasers.

**Keywords:** Ytterbium-doped, Phosphosilicate, High power, Fiber amplifier, Photo-darkening, Thermal characteristics.

**Student Number:** 2010-23280

# Contents

<b>Chapter 1. Introduction .....</b>	<b>1</b>
<b>Chapter 2. Yb-doped fiber lasers and amplifiers .....</b>	<b>4</b>
2.1 Principles of laser amplifiers .....	4
2.2 Ytterbium as a gain material .....	8
2.3 High power Yb-doped fiber laser amplifiers .....	10
2.4 Yb-doped phosphosilicate fiber and photo-darkening .....	12
<b>Chapter 3. Fiber spectroscopy and lifetime of the Yb-doped phosphosilicate fiber .....</b>	<b>13</b>
3.1 Absorption and emission cross-sections .....	14
3.1.1 Experiment setup of absorption and temperature dependent absorption cross-section.....	15
3.1.2 Experiment results .....	18
3.1.3 Experiment setup of temperature dependent emission cross-sections .....	20
3.1.4 Experiment results .....	21
3.1.5 Discussion on the temperature dependent cross-sections .....	22
3.2 Lifetime of Yb <sup>3+</sup> ions in phosphosilicate fiber.....	25
2.3.1 Experiment Setup.....	26
2.3.2 Experimental results .....	27
<b>Chapter 4. Temperature dependence of the Yb-doped phosphosilicate fiber laser amplifier .....</b>	<b>28</b>
4.1 Yb-doped phosphosilicate tunable fiber laser .....	29
4.2 Yb-doped phosphosilicate fiber laser amplifier .....	31
4.2.1 The amplifier efficiency.....	31
4.2.2 Noise of the amplifier .....	33
4.2.2 Temperature dependence of the amplifier.....	36

<b>Chapter 5. Conclusion.....</b>	<b>38</b>
<b>Bibliography .....</b>	<b>40</b>
<b>Abstract in Korean.....</b>	<b>42</b>

## **List of Tables**

Table 3.1 Absorption values of the Yb-doped phosphosilicate fiber at different wavelengths.....	19
Table 4.1 Output power trend of the Yb-doped phosphosilicate fiber amplifier with increasing temperature. ....	37

## List of Figures

Figure 2.1 Absorption and stimulated emission .....	4
Figure 2.2 Energy levels of a three-level and a four-level system .....	6
Figure 2.3 Electronic energy levels of the Yb <sup>3+</sup> ions in phosphosilicate fiber...	8
Figure 2.4 Cross-section and the end pumping of double-clad fibers.....	10
Figure 2.5 The MOPA scheme. ....	11
Figure 3.1 Experiment setup for the absorption measurement.....	15
Figure 3.2 The cutback method for the absorption measurement .....	15
Figure 3.3 Experiment setup for the temperature dependent absorption measurement .....	16
Figure 3.4 Transmission characteristic of the Yb-doped phosphosilicate fiber .....	18
Figure 3.5 Temperature dependent absorption cross-section. ....	19
Figure 3.6 Experiment schematic for the temperature dependent emission cross-section measurement.....	20
Figure 3.7 Temperature dependent emission cross-section.....	21
Figure 3.8 Differences in the absorption cross-section and the emission cross- section of the Yb-doped phosphosilicate fiber between 25 °C to 150°C .....	24
Figure 3.9 Lifetime measurement through backscattered signal.....	26
Figure 3.10 Change in lifetime with increasing temperature .....	27
Figure 4.1 Tunable seed laser based on the Yb-doped phosphosilicate fiber..	30
Figure 4.2 Output spectrum of the seed laser at different wavelengths .....	30
Figure 4.3 Fiber amplifier based on the Yb-doped phosphosilicate fiber .....	31
Figure 4.4 Output spectrum of the Yb-doped phosphosilicate fiber amplifier.. .....	32
Figure 4.5 Efficiency of the fiber amplifier at 1064 nm.....	32
Figure 4.6 Noise figure of the Yb-doped phosphosilicate fiber amplifier.....	35
Figure 4.7 Trend of the fiber amplifier output power with increasing temperature.....	37

# Chapter 1. Introduction

Fiber laser amplifier is a device which provides amplification of light with an optical fiber as a gain medium. The optical fiber is usually doped with rare-earth materials such as ytterbium, erbium, neodymium, and thulium. In 1986, an optical fiber having erbium-doped core was demonstrated to amplify telecommunication signal efficiently by David Payne of the University of Southampton [1]. It is now widely known as erbium doped fiber amplifier (EDFA). Since then, the interest and effort exploded in the field with the growing social demand for the telecommunication. Also, possibilities of fiber laser amplifiers have been intensively researched for various applications.

High power fiber amplifier is one of the most important applications of fiber amplifiers [2]. Ever since reaching the remarkable milestone of the first kilowatt fiber laser in 2004 [3], output of multiple kilowatts have been made available through high power fiber amplifiers based on ytterbium-doped double-clad fibers [4]. With ever increasing output power through different technical approaches, efforts and tradeoffs have been made in order to overcome the obstacles to achieve a desired level of high power operation.

Power in the fiber lasers and amplifiers are usually limited by physical damage threshold of the silica fiber material and nonlinearities experienced by the fiber when operating above the nonlinear threshold. To deal with these problems, adapting larger core size or increasing the rare-earth doping level is the considerable measure [5]. However, controlling the doping level is more desirable for beam quality perspective rather than playing with the core size.

By increasing the rare-earth doping level in a gain medium, higher power can be achieved with higher nonlinearity threshold and shorter fiber length. However, increasing the rare-earth doping level also has trade-offs. At high rare-earth doping level, a fiber is subject to concentration quenching, reduced lifetime and photo-darkening (PD) [6]. Among these drawbacks from high rare-earth concentration, photo-darkening may be the most detrimental in a sense that normally this effect will permanently degrade the fiber laser efficiency.

Photo-darkening is a phenomenon where absorbing color centers are created in a silicate glass composite optical fiber upon incident light [7]. Photo-darkening is known to be related with the number density of excited ions and high level of clustering induced by it. The exact mechanism for its appearance is still in debate. Some believe that it is due to ytterbium clusters bridging up the energy band gap of the silicate host and some believe that it results from the unstable valence band state of ytterbium ions inside of the silicate glass matrix [8].

Ytterbium-doped phosphosilicate fibers are known to provide higher solubility for ytterbium ions in silica glass host and proved to be more resistant to photo-darkening compared to aluminosilicate based ytterbium-doped fibers. Not only phosphosilicate-based ytterbium-doped fibers demonstrate higher photo-darkening resistance [9], it also has substantially longer lifetime compared to aluminosilicate-based fibers and higher damage threshold than the phosphate glass fibers. Even though ytterbium-doped phosphosilicate fiber has a drawback of lower absorption cross-section for transitions between  ${}^2F_{5/2}$  and  ${}^2F_{7/2}$ , it is still a great option as a gain medium in

high power regime for its outstanding characteristics especially high resistance against the photo-darkening.

In the thesis, the author presents thermal characteristics of an ytterbium-doped phosphosilicate fiber based on experimental results. The principles behind ytterbium-doped fiber laser amplifier are discussed in Chapter 2. Chapter 3 deals with the characterization of the fiber itself. A tunable amplifier based on this fiber is characterized and temperature dependent experimental results are shown in Chapter 4 and Chapter 5 concludes the thesis.

## Chapter 2. Yb-doped fiber lasers and amplifiers

### 2.1 Principles of laser amplifiers.

An optical amplifier relies on the theory of LASER, Light Amplification by Stimulated Emission of Radiation, to amplify light [10]. The amplitude of optical input field is amplified with original phase remaining still. Even though the word ‘laser’ is normally perceived and used as a light emitting device producing coherent and monochromatic light, it is actually a concept of light amplification [11]. Figure 2.1 shows absorption and stimulated emission which are responsible for attenuation and gain respectively.

In stimulated emission, a photon induces an electron in an upper energy level to go down to a lower energy level while inducing the electron to emit a clone photon of the same mode. In absorption process, an electron in a lower level absorbs photon energy to excite to the upper energy level.

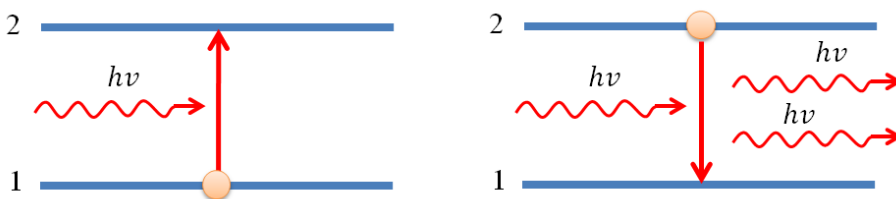


Fig 2.1 Absorption and stimulated emission.

However, for an optical amplifier to have gain, the condition of population inversion shown in Eq. (2.1), where  $N_2$  and  $N_1$  denote the number of atoms in each energy level, needs to be satisfied.

$$N > 0 \quad (2.1)$$

$$N = N_2 - N_1 \quad (2.2)$$

To achieve population inversion, adequate amount of external pump power needs to be supplied to the gain medium. If the population inversion is reached, photon absorption process which results in attenuation can be overcome with stimulated emission achieving net gain in the amplifier. The gain coefficient of an amplifier is represented as Eq. (2.3), where  $\sigma(\nu)$  is the transition cross-section,  $t_{sp}$  is the spontaneous lifetime, and  $g(\nu)$  is the normalized lineshape function [12].

$$\gamma(\nu) = N\sigma(\nu) = N \frac{\lambda^2}{8\pi t_{sp}} g(\nu) \quad (2.3)$$

Lasers, depending on gain medium, require different pumping schemes [13]. Figure 2.2 shows energy levels of a three-level system and a four-level system, where  $R$  is the pump rate,  $W^{-1}$  is the probability density of absorption and stimulated emission, and  $t$  is the lifetime of different transitions among sublevels. Inverse of the lifetime is decay rate,  $\tau$ , of each transition.

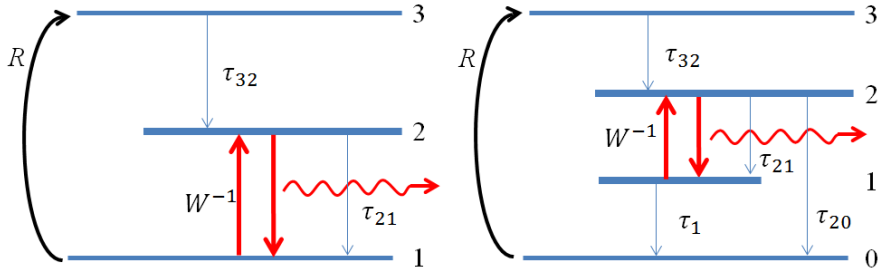


Fig 2.2 Energy levels of a three-level and a four-level system.

In case of three-level system, population of atoms in energy level one, the ground state, is externally pumped up to the short-lived energy level three. The excited atoms then quickly fall down and accumulate the long-lived energy level two. The laser transition occurs by atoms dropping to the energy level one from the energy level two. It requires relatively high pump threshold because at least the half of the atoms need to be excited above the ground level to maintain the population inversion. The four-level system differs from the three-level system that it has an additional state between the energy level two and the ground state. Lasing transitions are held between the energy level two and a short-lived energy level one. The four-level system requires less pump power because its lower lasing energy level depopulates quickly unlike the three-level system.

Another interesting energy system is the quasi-three-level system. The quasi-three-level system can be thought of something in between the three-level system and the four-level system [14]. When the lower level of the lasing energy level is very close to the ground state, population tend to build up in this level due to the operation temperature causing reabsorption and reduced gain. Ytterbium-doped gain media represents the quasi-three-level

system [15]. In case of Yb-doped silica fibers, wavelength below 1040 nm operates almost like a three-level system. While the system acts nearly like the four-level system beyond 1080nm. It is possible to conclude that operation characteristics including the laser efficiency are more subject to temperature change in quasi-three-level systems because of the ease of the sublevel transitions in lower lasing level compared to the other systems. In this thesis, thermal characteristics of the Yb-doped phosphosilicate fiber amplifier are studied at the wavelengths of 1060nm, 1070nm and 1080nm, where the system is known to operate as a quasi-three-level system.

## 2.2 Ytterbium as a gain material

Ytterbium is the predominant choice of rare-earth dopant in gain medium of high power optical fiber amplifiers. Normally it is doped as a trivalent form of  $\text{Yb}^{3+}$  in silicate glasses or crystals. There are couple characteristics that help ytterbium to stand out as an efficient doping material [16].

$\text{Yb}^{3+}$  ions have very simple energy level structure which frees ytterbium from experiencing excited-state absorption. Excited-state absorption tends to occur in materials with more complicated electronic levels where the pump or the laser radiation is brought up to a higher electronic level resulting in lower slope efficiency and lasing offset. Figure 2.3 shows the electronic level structure of the  $\text{Yb}^{3+}$  ions in a phosphosilicate fiber. Unlike the multi-level structured materials, sublevels in the upper-state,  $^2\text{F}_{5/2}$ , and ground-state,  $^2\text{F}_{7/2}$ , hold all the transitions regarding pump and amplification.

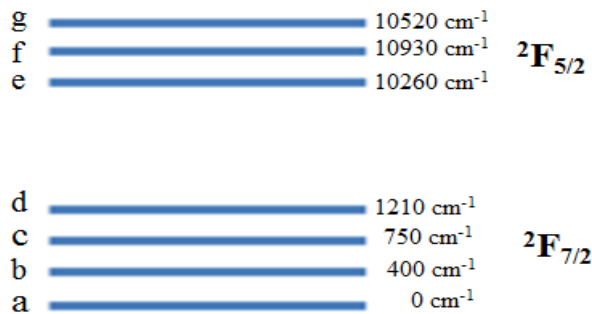


Fig 2.3 Electronic energy levels of the  $\text{Yb}^{3+}$  ions in phosphosilicate fiber.

Not only ytterbium has simple electronic structure, it is very suitable material for high power lasers and amplifiers because of its small quantum defect. Quantum defect defined in Eq. (2.1), where  $\omega_p$  is the pump frequency and  $\omega_s$  is the lasing frequency, refers to pump energy lost in the gain medium failing to lase. High quantum defect can cause thermal control issues and in turn lower laser efficiency [17].

$$q = \hbar\omega_p - \hbar\omega_s \quad (2.4)$$

Ytterbium also presents other desirable aspects such as large gain bandwidth and relatively longer upper-state lifetime which are favorable for different applications such as mode-locked lasers and tunable lasers.

## 2.3 High power ytterbium-doped fiber laser amplifiers

In most cases, high power fiber lasers are based on double-clad fibers doped with rare-earth materials such as ytterbium. Such fiber can achieve both high quality beam and high power through cladding pumping where the laser signal is guided in the core while pump light travels through the large inner cladding causing excitation in the active medium. Figure 2.4 shows an example of a double-clad fiber. Double-clad Yb-doped fibers are composed of an Yb-doped core, a normally anti-symmetry shaped inner-cladding for pump guiding and an outer-cladding with the lowest refractive index [18]-[20].

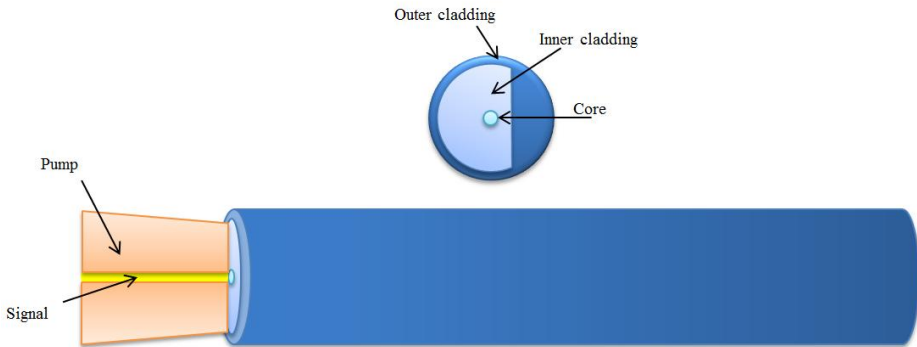


Fig 2.4 Cross-section and the end pumping of double-clad fibers.

Taking advantage of double-clad fibers and ytterbium, a highly promising dopant for high power application, master oscillator power amplifier (MOPA), a combination of laser and amplifier stages, can be built.

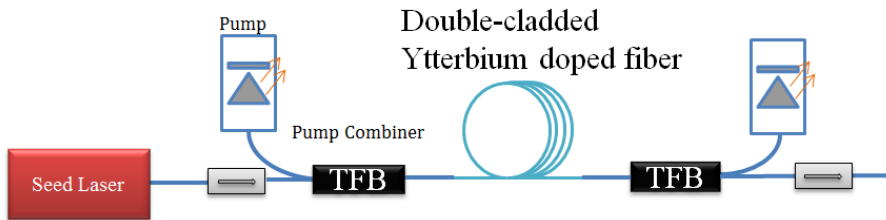


Figure 2.5 The MOPA scheme.

MOPA system provides great beam quality, emission controllability and high power efficiency. In the thesis, a tunable fiber laser is built using the Yb-doped phosphosilicate fiber and a single stage of amplifier is built with the same fiber for thermal characteristic experiment.

## **2.4 Yb-doped phosphosilicate fiber and photo-darkening.**

Highly Yb-doped fibers especially for high power applications where high excitation density is required to mitigate nonlinear effects, often experience a gradual degradation of laser performance through formation of unwanted broadband absorption near visible light and infrared called photo-darkening. The underlying mechanism behind photo-darkening is still in debate. Koponen observed that growing rate of the loss to be proportional to the seventh power of the ion inversion. Morasse suggested the generation of UV-photons from de-excitation of Yb-ions. The unstable nature of valence state in Ytterbium ions in silica matrix contributing to photo-darkening was also suggested by Engholm [7]-[9].

The material composition and the homogeneity of the active gain matrix control the appearance of the photo-darkening. It is understood from previous study that an aluminosilicate based Yb-doped fibers exhibit charge-transfer (CT) band near 230 nm. The excitation into this band generates color center and it becomes part of photo-darkening process. By changing the glass composition, for example to a phosphosilicate based Yb-doped fiber, the CT band is shifted to shorter wavelength and resulted in much lower loss under 915 nm high power pumping [8].

Even though Yb-doped phosphosilicate fiber exhibit stronger photo-darkening resistance, it has smaller absorption cross-section compared to aluminosilicate fiber. However tradeoffs need to be made in many cases. Yb-doped phosphosilicate fiber is a desirable option for high power application with reduced photo-darkening, longer lifetime, and higher damage threshold.

## **Chapter 3. Fiber spectroscopy and lifetime of the Yb-doped phosphosilicate fiber**

Fiber spectroscopy and the lifetime measurement are important steps before setting up the fiber lasers and amplifiers. Fiber spectroscopy in this case, absorption cross-section and emission cross-section provides us with information of the fiber, in which wavelength the fiber will absorb and emit light. It is fair to say the fiber spectroscopy of the laser tells you the most about the laser built around it. Yb-doped phosphosilicate fibers are known to have noticeable absorption band over 940 nm unlike aluminosilicate based fibers. Measuring the lifetime of ions in a fiber is also important. Lifetime of the ytterbium ions in the fiber is directly related with the gain efficiency and the threshold pump power.

In this chapter, the absorption cross-section and the emission cross-section are measured along with the fluorescence lifetime. Temperature dependent characteristics are also measured and analyzed.

### 3.1 Absorption and emission cross-sections.

Transition cross-sections are very important characteristics of a fiber as a gain medium. The name sounds like an area or a geometric size. However, it is actually a function of absorption or emission efficiency or strength along the wavelength. The probability of each ground state carrier being pumped into the metastable state every second is given in Eq. (3.1) where  $P_p$  is the pump power,  $f_p$  is the pump frequency, and  $A$  is the effective fiber core cross-section area. Consequently, it is possible to define the absorption cross-section as the ratio of pump absorption efficiency and the density of pump photon flow rate as shown Eq. (3.2). Similarly, the emission cross-section is given in Eq. (3.3) where  $P_s$  denotes the emitted signal power,  $f_s$  is the frequency of the signal and  $W_s$  is the stimulated emission efficiency [21].

$$W_p = \frac{\sigma_a P_p}{h f_p A} \quad (3.1)$$

$$\sigma_a = W_p / \left( \frac{P_p}{h f_p A} \right) \quad (3.2)$$

$$\sigma_e = W_s / \left( \frac{P_s}{h f_s A} \right) \quad (3.3)$$

### 3.1.1 Experiment setup of the absorption and the temperature dependent absorption cross-section.

The absorption of the Yb-doped phosphosilicate fiber was measured using the experiment setup shown in Fig 3.1. White light source was used as a reference signal. Lenses were placed to collimate the beam into the Yb-doped phosphosilicate fiber for its diameter was greater than 125  $\mu\text{m}$  and bare fiber connector fitting this fiber was not present at the moment. The output signal after the fiber was measured using the cutback method shown in Fig 3.2.

In the cutback method, the absorption of 5 m of the fiber was measured first. 1 m of the fiber from the original fiber was then cut and measured again. The measurements were taken for every 1 m of the fiber cut. Each measurement is compared to the others and the original reference signal.

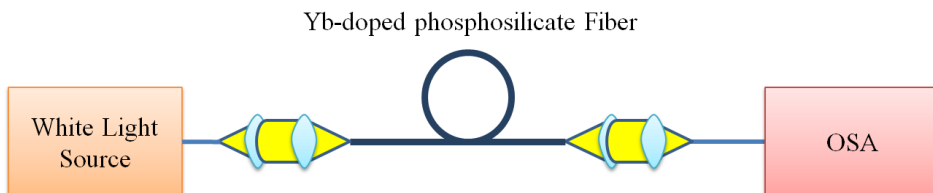


Fig 3.1 Experiment setup for the absorption measurement.

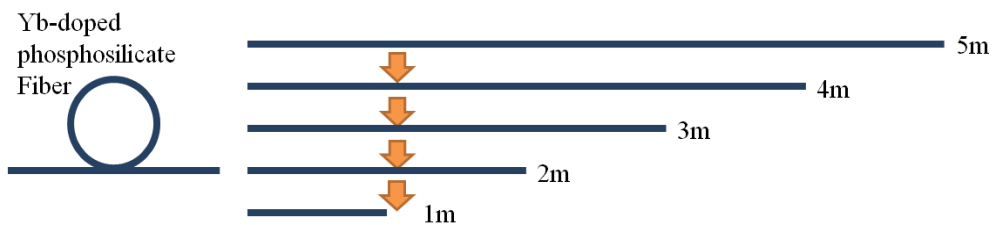


Fig 3.2 The cutback method for the absorption measurement.

The absorption cross-section was also measured with increasing temperature to understand its behavior with temperature variation. Again, white light source was used as a reference signal and the Yb-doped phosphosilicate fiber was placed inside a temperature-controlled oven. Each side of the Yb-doped phosphosilicate fiber was spliced to a single-mode fiber. The output signal was measure with optical spectrum analyzer. The experiment schematic is shown in Fig. 3.3.

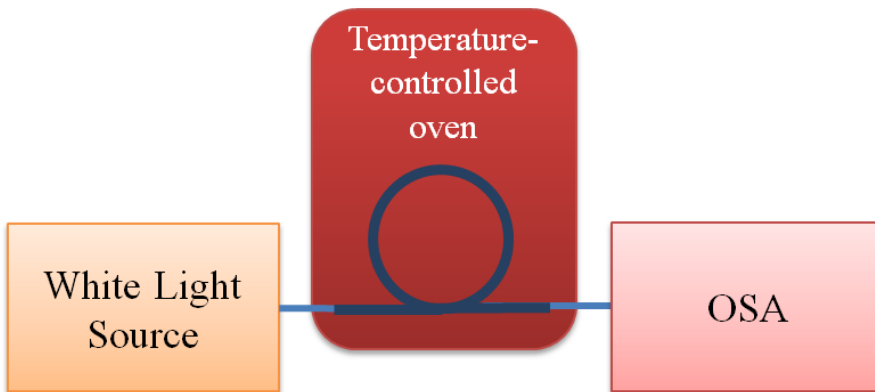


Fig 3.3 Experiment setup for the temperature dependent absorption measurement.

### 3.1.2 Experiment results

Figure 3.4 represents the transmission characteristic of the Yb-doped phosphosilicate fiber. There are three wavelengths where the absorptions were noticeable, 915 nm, 940 nm, and 975 nm. The average absorptions at these peaks were given in Table 3.1. At 915 nm, the average absorptions were 0.308 dB, 0.334 dB, and 2.13 dB at 915 nm, 940 nm and 975 nm respectively.

Temperature dependent absorption cross-section is given in the Fig. 3.5. As we started to increase the temperature, absorption peaks decreased in the region of available pump windows of 915nm, 940nm and 975nm for Yb-doped phosphosilicate fiber. The peaks and valleys of absorption and emission spectra correspond to different transitions among the stark levels. Yb<sup>3+</sup>-ion population at the each stark level changes according to the Boltzmann distribution. As temperature increases, the upper levels of each stark level in Yb<sup>3+</sup>-ion energy levels,  $^2F_{5/2}$  and  $^2F_{7/2}$ , will populate more, this in turn reduces the population in the lower level. As temperature increases, the populations in the lowest levels decrease while those in the upper levels increase.

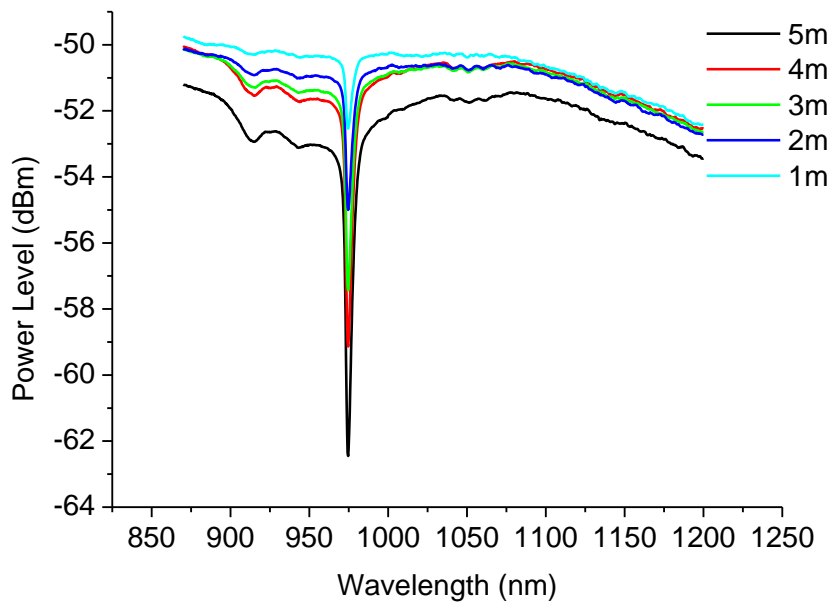


Fig 3.4 Transmission characteristic of the Yb-doped phosphosilicate fiber.

Table 3.1 Absorption values of Yb-doped phosphosilicate fiber at different wavelengths.

Fiber length	$\alpha@915$ nm	$\alpha@940$ nm	$\alpha@975$ nm
5 m to 4 m	0.31 dBm	0.28 dBm	2.29 dBm
4 m to 3 m	0.29 dBm	0.36 dBm	1.27 dBm
3 m to 2 m	0.37 dBm	0.42 dBm	2.42 dBm
2 m to 1 m	0.26 dBm	0.28 dBm	2.12 dBm
Average	0.308 dBm	0.334 dBm	2.13 dBm

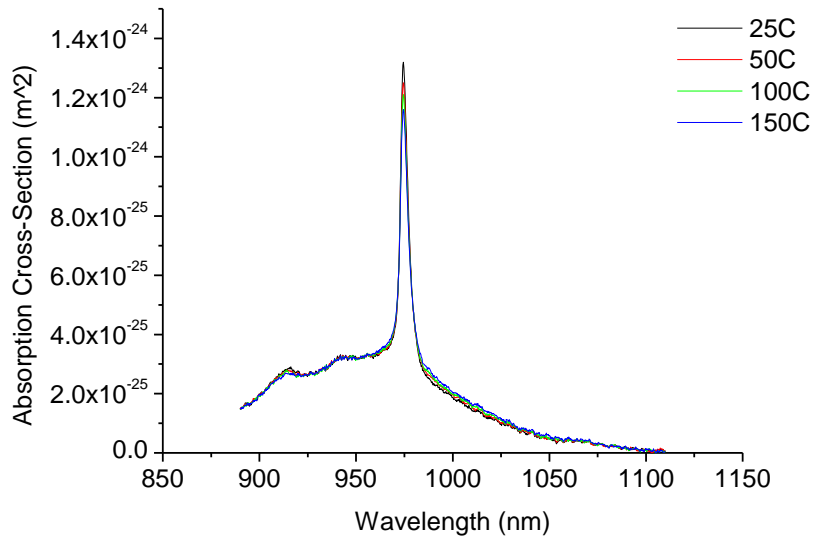


Fig 3.5 Temperature dependent absorption cross-section.

### 3.1.3 Experiment setup of the temperature dependent emission cross-section

To obtain the emission cross-section, the back scattered signal from one of the multimode ports of the power combiner was measured. The schematic of the experiment is shown in Fig. 3.6. Laser diode operating at 915 nm was controlled by the Laser diode driver. The pig tail of the laser diode was spliced to a power combiner where the output was again spliced to a short piece of the Yb-doped phosphosilicate fiber, in this case 1 m. The reason for choosing such short length of the fiber was to avoid reabsorption of the ytterbium ions. The Yb-doped phosphosilicate fiber was then placed inside of the temperature-controlled oven. One of the multimode ports was connected to the optical spectrum analyzer.

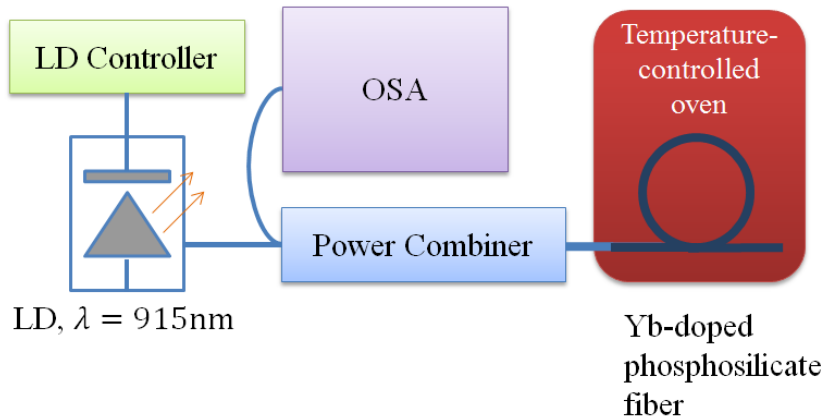


Fig 3.6 Experiment schematic for temperature dependent emission cross-section measurement.

### 3.1.4 Experimental results

The emission cross-sections at different temperatures are given in Fig.3.7. The measurement of emission cross-section was taken from room temperature to 150 °C. It is clear that the emission decreases in all the peaks while some of the valleys grow at higher temperature. The most noticeable differences can be found at 975nm, 1025nm and 1060nm. Again, the peaks and valleys of the emission spectrum correspond to different transitions among the stark levels. This phenomenon explains the change of fluorescence lifetime along the increasing temperature. More detailed analysis on relations among each transition and peaks and valley requires through quantum mechanical approach.

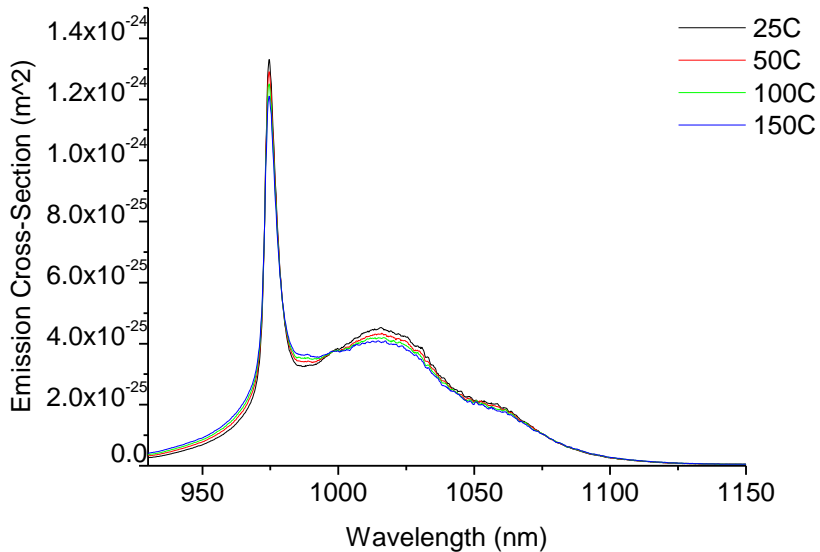


Fig 3.7 Temperature dependent emission cross-section.

### 3.1.5 Discussion on the temperature dependent cross-sections

It is important to understand the energy levels of  $\text{Yb}^{3+}$  ions in the fiber to relate the changes witnessed in the transition cross-sections. The electronic structure of  $\text{Yb}^{3+}$  ions has two manifolds, the ground state  $^2\text{F}_{5/2}$  and the excited state  $^2\text{F}_{7/2}$ . Each state is split into Stark sublevels where the ground state  $^2\text{F}_{5/2}$  has four sublevels from a to d and the excited state  $^2\text{F}_{7/2}$  has three sublevels from e to g as shown in the Fig. 2.3. Each of the sublevels has different energy depending on the composition of the fiber. It is known to be greatly affected by the host material. In case of aluminosilicate based ytterbium doped fiber, the energy levels differed about  $200\text{ cm}^{-1}$  to  $500\text{ cm}^{-1}$ .

The energy levels of  $\text{Yb}^{3+}$  ions and the transition among the sublevels have close relationship with the absorption and emission cross-sections. The noticeable peaks and valleys of the cross-sections represent different transitions among the energy levels. First by taking a look at the absorption cross-section, the peaks observed around 900 nm to 950 nm including the peak at 940 nm indicate the sublevel transition from  $a \rightarrow f$  and  $a \rightarrow g$ . The main peak observed around 974 nm corresponds to  $a \rightarrow e$  transition. Transitions from b to upper levels represent absorptions at longer wavelengths of 1030 nm to 1200 nm. In the emission cross-section, the main peak found at 975 nm corresponds to the most likely transition of  $e \rightarrow a$ . Less likely transitions considering the moderate thermal condition,  $e \rightarrow b$ ,  $e \rightarrow c$ , and  $e \rightarrow d$  correspond to emissions peaks in the range of 1030 nm to 1200 nm. Meanwhile some of the valleys in the cross section also represent transitions in the sublevels. Valley near 960 nm is known to represent the transition from

$f \rightarrow b$  and  $b \rightarrow f$ .

With the idea of such relation in mind, it is possible to understand the cross-section change induced by different thermal conditions. The general trend noticed in both absorption and emission cross-section was that the peaks reduced and the valleys representing weaker transitions grow noticeably as temperature was increased from 25 °C to 150 °C. The  $\text{Yb}^{3+}$ -ion populations in the sublevels are governed by the Boltzmann distribution. As temperature increases, the upper levels of each Stark level in  $\text{Yb}^{3+}$ -ion energy levels,  $^2F_{5/2}$  and  $^2F_{7/2}$ , will populate more, this in turn reduces the population in the lower level. This phenomenon is clearly explained with the experiment result. From the absorption and emission cross-sections, all the peaks corresponding to the lowest Stark level transitions decreased. The population at these levels reduced as temperature increased according to the Boltzmann distribution. Meanwhile, the valley referring to  $f \rightarrow b$  and  $b \rightarrow f$  grew with increasing temperature. Temperature increase caused ion population transfer among these Stark levels and resulted in cross-section change which in turn will explain the degradation in the amplifier performance.

The difference between cross-sections at 25 °C and 150 °C is shown in Fig. 3.8. Thermal effect depending on the wavelength can be inferred from this graph. For absorption cross-section, there was clear decrease around the wavelength of 920 nm, 950 nm, and 974 nm. These wavelengths refer to the absorptions from the lowest level of the ground manifold. Increase in the cross-section was observed around the wavelength of 970 nm and longer wavelengths. They represent upper level transitions such as  $b \rightarrow f$  and  $c \rightarrow g$ . In the emission difference graph, similar to the difference in absorption, the

lower Stark level transitions decreased while the valleys representing upper Stark level increased. An important point to note is the increasing cross-section difference in emission while decreasing trend in absorption cross-section difference near 1060 nm to 1080 nm.

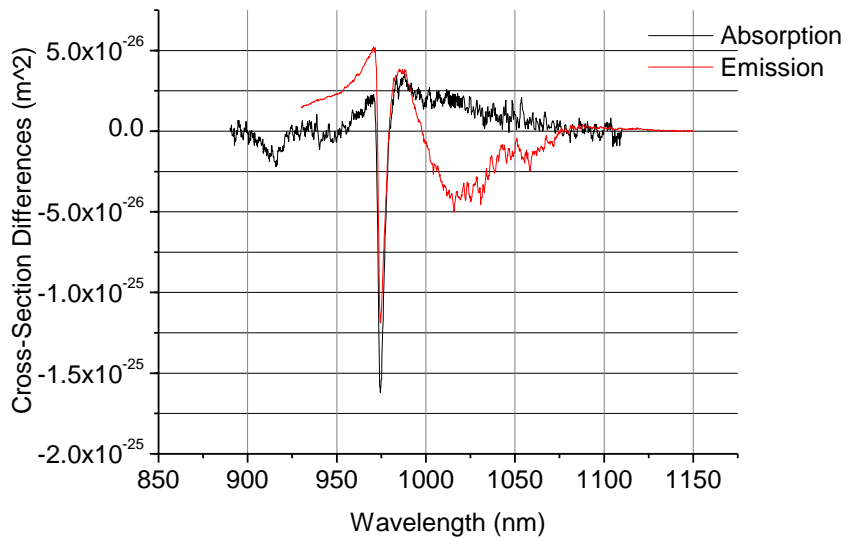


Fig 3.8 Differences in the absorption cross-section and the emission cross-section of the Yb-doped phosphosilicate fiber between 25 °C to 150°C.

## 3.2 Lifetime measurement of Yb<sup>3+</sup> ions in phosphosilicate fiber

In an amplification process, excited populations emit clone photons and decay into lower energy level by stimulated emission. However, stimulated emission is not the only process that brings the excited ions into the ground state. Spontaneous emission is the main factor defining the lifetime of the ions at the upper-state level. The upper state lifetime is often defined by the inverse lifetime in Eq. (3.4) [22].

$$\frac{1}{\tau_{rad}} = \frac{8\pi n^2}{c^2} \int \nu^2 \sigma_e(\nu) d\nu \quad (3.4)$$

Lifetime is a crucial factor in choosing a laser gain medium. A longer upper-state lifetime means that less pump power is needed to maintain population inversion. Relaxation oscillation and spiking tendency are also known to be influenced by lifetime of the gain medium.

The life time of Yb<sup>3+</sup> ions in phosphosilicate fiber is measured in this section. The experiment setup and the results along with the temperature dependent characteristic are discussed.

### 3.2.1 Experiment Setup

Experiment setup for the lifetime measurement of ytterbium ions in the fiber is shown in Fig. 3.9. Because the fiber had to be placed inside of the temperature-controlled oven, the side detection method could not be used. The lifetime was measured with back scattered signal. The pump diode operating at 915 nm was driven in pulsed mode with 10 Hz repetition rate and 10 % duty cycle. The pump duty cycle and the pump intensity of 1.5 W were chosen to ensure that all the  $\text{Yb}^{3+}$  ions are excited. The pig-tailed diode was spliced to a power combiner where the output port is spliced to 50 cm of the Yb-doped phosphosilicate fiber placed inside a temperature-controlled oven. The second power combiner was spliced to the input of the first power combiner to maximize the backscattered light to the photodiode. The dichroic mirror was placed to block the pump power at 915 nm going into the photodiode. Measurements were taken at 25°C, 50°C, 100°C and 150°C.

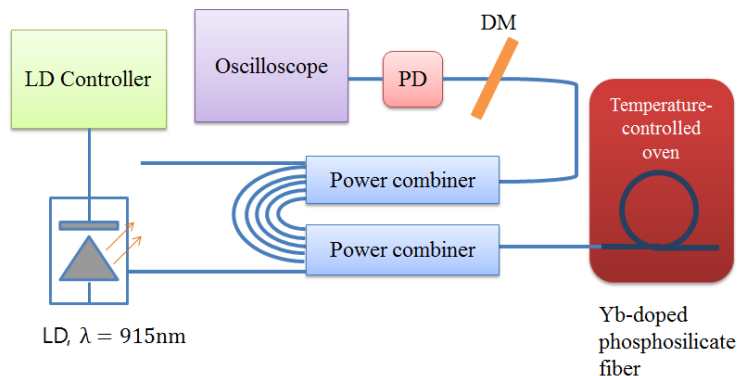


Figure 3.9 Lifetime measurement through backscattered signal.

### 3.2.2 Experimental results

The lifetime of the Yb-doped phosphosilicate fiber decreased from 1.502 ms at 25°C to 1.479 ms at 150°C. The trend of decreasing lifetime along with increasing temperature of the fiber is shown in Fig. 3.10. The lifetime of the Yb-doped phosphosilicate fiber at room temperature was substantially longer than aluminosilicate based Yb-doped fibers. Aluminosilicate based fibers are known to have lifetime of less than 1 ms. Even though the lifetime change was not significant, the decreasing trend is clear and it is possible to conclude that the overall variation in energy level transitions due to the temperature change according to the Boltzmann's distribution has caused the lifetime to decrease with increasing temperature.

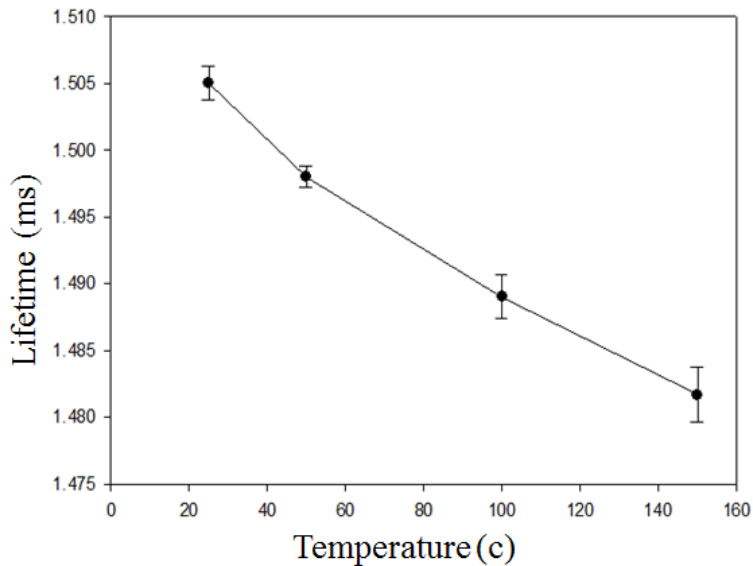


Figure 3.10 Change in lifetime with increasing temperature.

## **Chapter 4. Temperature dependence of the Yb-doped phosphosilicate fiber laser amplifier**

Information of temperature dependent characteristics of a fiber is crucial when modeling a fiber laser or a fiber amplifier system. These characteristics play even greater role in high power regime where the operating temperature is normally higher than that of the lower power regime. In this chapter, the thermal characteristics of a fiber amplifier based on the Yb-doped phosphosilicate fiber are studied. First the Yb-doped phosphosilicate tunable fiber laser was setup as seed and the amplifier stage is discussed after the seed laser. Not only the thermal characteristics, noise property and output power depending on different wavelengths of the amplifier are also discussed.

## **4.1 Yb-doped phosphosilicate tunable fiber laser**

Before being able to test the thermal characteristics of the fiber amplifier, a seed laser was required. Figure 4.1 shows the schematic of the tunable seed laser. Laser diode operating at 915 nm was used to pump 13 m of the Yb-doped phosphosilicate fiber. Isolators were placed inside of the cavity to ensure unidirectional operation of the ring laser. High-Index gel (HI Gel) was applied at the splice point between the Yb-doped phosphosilicate fiber and the isolator to ensure the pump power remaining after the gain medium does not go through the remaining cavity. For wavelength selection, a manual fiberized filter was placed inside of the cavity. Figure 4.2 represents the output spectrum measured at the 30% coupler output. The laser was set to output 150 mW at different wavelengths. The output at 1040 nm and 1050 nm contained noticeable ASE.

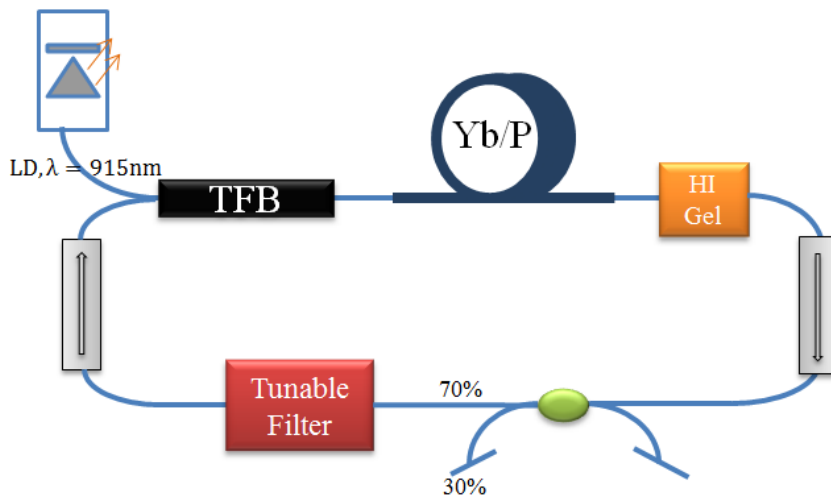


Figure 4.1 Tunable seed laser based on the Yb-doped phosphosilicate fiber.

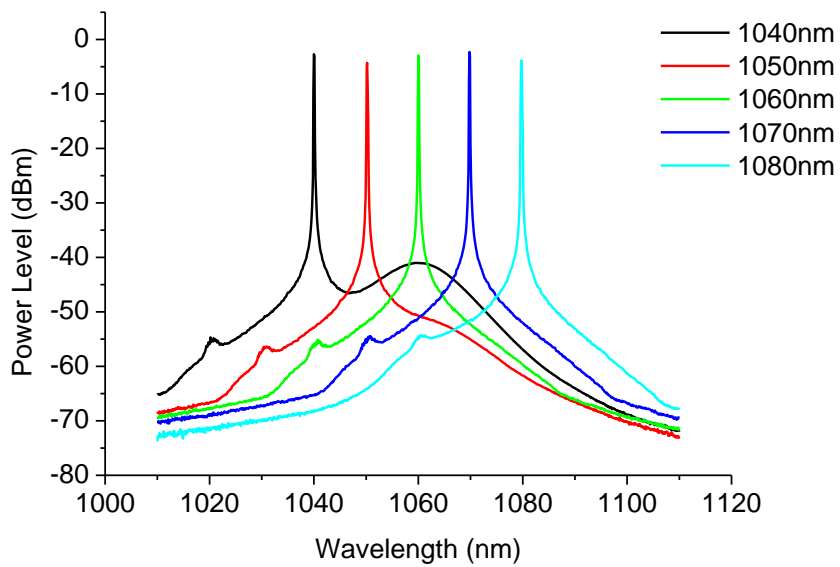


Figure 4.2 Output spectrum of the seed laser at different wavelengths.

## 4.2 Yb-doped phosphosilicate fiber laser amplifier

### 4.2.1 The amplifier efficiency.

With the seed laser ready, the Yb-doped phosphosilicate fiber laser amplifier was setup as the schematic shown in Fig. 4.3. The seed laser was spliced to a coupler to monitor the input signal to the amplifier stage. For the amplifier stage, laser diode operating at 940 nm was used to pump the Yb-doped phosphosilicate fiber. The length of the fiber was chosen to be 33 m to obtain 10 dB absorption. Dichroic mirror was placed to separate the output signal and the unabsorbed signal. Figure 4.4 shows the output spectrum of the fiber amplifier at 1060 nm, 1070 nm and 1080 nm. The amplifier efficiency was 68.5 % as shown in the Fig. 4.5.

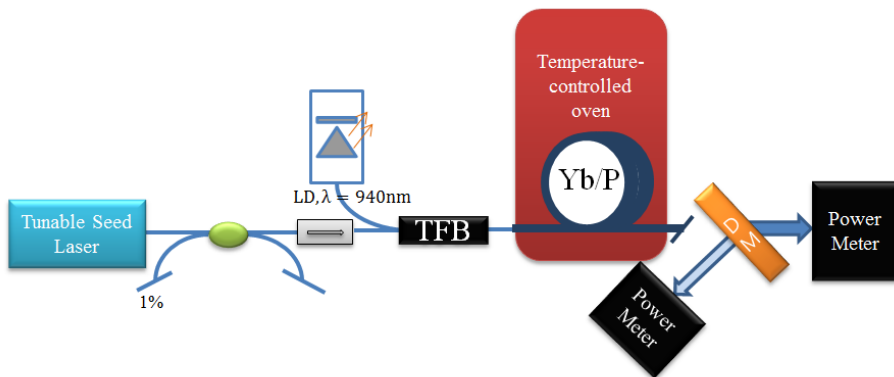


Figure 4.3 Fiber amplifier based on the Yb-doped phosphosilicate fiber.

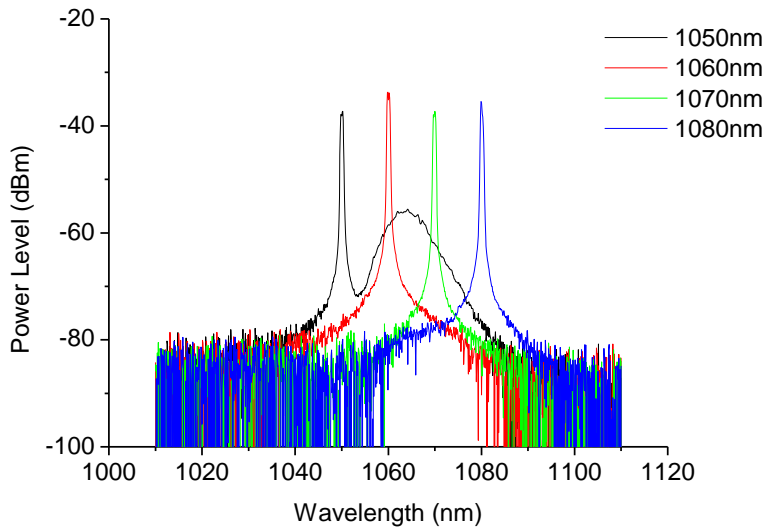


Figure 4.4 Output spectrum of the Yb-doped phosphosilicate fiber amplifier.

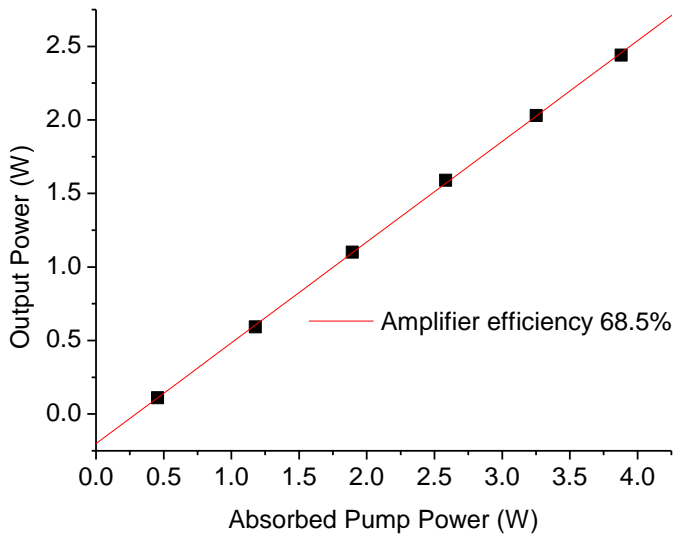


Figure 4.5 Efficiency of the fiber amplifier at 1064 nm.

### 4.2.2 The Noise of the amplifier.

In an optical amplifier, not only the signal from the stimulated emission, but also the photons from the spontaneous emission are amplified. These amplified photons generated by the spontaneous emission are considered to be noise and they are named as the amplified spontaneous emission (ASE). Noise figure shown in Eq. (3.5) as the ratio between the input signal to noise ratio (SNR) to the output SNR represents how much excess noise has been added to the original signal after going through the fiber amplifier [23].

$$F_o = \frac{SNR_o(0)}{SNR_o(z)} \quad (3.5)$$

In an optical amplifier, noise figure can be expressed as a function of noise spectral density given in Eq. (3.6) where  $n_{sp}$  denotes the unit less spontaneous emission factor.

$$\rho(\lambda) = 2n_{sp} \frac{hc}{\lambda} [G(\lambda) - 1] \quad (3.6)$$

$$F_o = \frac{\lambda\rho}{hcG} + \frac{1}{G} \quad (3.7)$$

Theoretical noise figure assuming a shot noise limited, a fundamental limit to the optical intensity noise, input signal is given in Eq. (3.8) [24].

$$NF_{ideal} = 1 + \frac{|G-1|}{G} \quad (3.8)$$

The measurement of noise figure of the amplifier at 10 dB gain was taken using the optical method through optical spectrum analyzer and interpolation. Figure 4.6 shows the noise figure of 33 m and 22m of the Yb-doped phosphosilicate fiber laser amplifiers as red and blue dot respectively. Input signal of 150 mW was seeded into both amplifiers for 10 dB gain. The theoretical noise figure was graphed on the same plot for comparison. The experimental values and the theoretical values show some discrepancies. This results from reabsorptions at 1064 nm owing to the quasi three-level structure of the Yb-doped fiber amplifiers.

Amplifiers with different gain medium lengths were experimented to understand the relationship between the reabsorption and the noise figure. Noise figures of the fiber amplifier at 10 dB gain for 33 m and 23 m were 5.8 dB and 5.1 dB respectively. Pump power required to maintain the same gain level is greater for shorter fibers because it will absorb less. In the process, reabsorption will decrease with fiber length resulting in improved noise figure. Even though there are trade-offs of pump power and gain level, by using shorter fiber one can improve the noise figure of the Yb-doped phosphosilicate fiber.

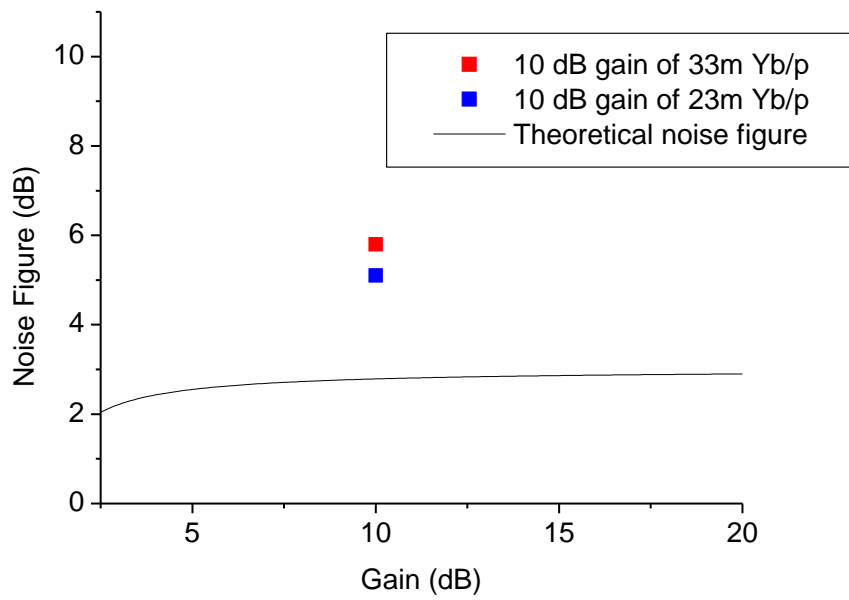


Figure 4.6 Noise figure of Yb-doped phosphosilicate fiber amplifier.

### **4.2.3 The temperature dependent output of the amplifier.**

Temperature dependent characteristics of the amplifier was measured by setting the seed laser generating signal of 150 mW to the amplifier stage and amplifier was pumped to achieve the 10 dB gain of output 1.5 W at all three wavelengths. Output power and unabsorbed pump power were measured with power meters at 25 °C, 50 °C, and 100 °C respectively. The output of the amplifier at three different wavelengths with increasing temperature are given in Table 4.1. The table clearly shows that with increasing temperature, the output power degrades noticeably. The output power decreased 19.3 % compared to room temperature output at 1060 nm when the amplifier is operating at 100 °C. The trend of decreasing output with increasing temperature is represented in Fig. 4.7. The general trend in the power degradation was similar to the aluminosilicate based Yb-doped fiber amplifier where the order of wavelength dependent output power could be explained with the difference in the fiber spectroscopy between the room temperature and 100 °C. In the wavelength range of 1060 nm and 1080 nm, the emission cross-section shows decreasing trend as the wavelength increases which means that near 1060 nm the emission experienced greater decay with increasing temperature. Meanwhile the absorption cross-section difference shows that there is more absorption at 1060 nm compared to 1070 nm and 1080nm, meaning that the greater power degradation at lower wavelength have been caused by higher re-absorption at these wavelengths.

Table 4.1 Output power trend of the Yb-doped phosphosilicate fiber amplifier with increasing temperature.

	@1060 nm	@1070 nm	@1080 nm
$P_{RT}$	1.50 W	1.50 W	1.50 W
$P_{50}$	1.34 W	1.38W	1.44W
$P_{100}$	1.21W	1.25W	1.36W
$P_{100}/ P_{RT}$	0.807	0.833	0.907
Degradation	19.3%	16.7%	9.3%

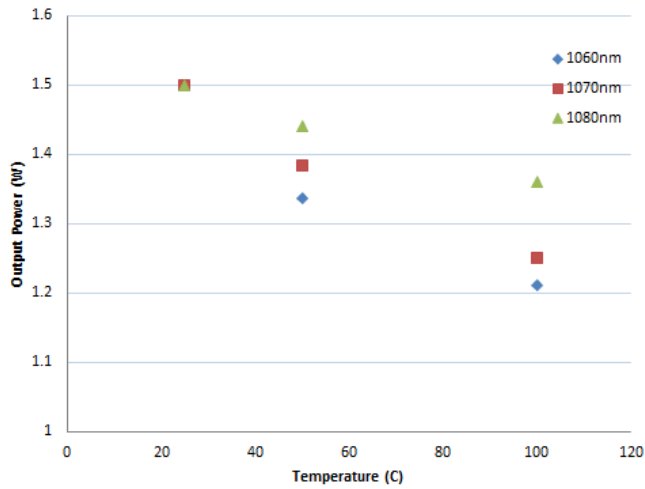


Figure 4.7 Trend of fiber amplifier output with increasing temperature.

## Chapter 5. Conclusion

Ytterbium-doped phosphosilicate fibers demonstrating high photo-darkening resistance, longer lifetime, and higher damage threshold is a great option for a gain material in high power fiber lasers and amplifiers. Hence it is worth studying the temperature dependence of this fiber for applications in high power regime.

In the thesis, characterization of the Yb-doped phosphosilicate fiber was conducted. The absorption cross-section, the emission cross-section, and the lifetime of the fiber were found including their temperature dependence. After the characterization of the fiber, a tunable fiber laser and a fiber laser amplifier based on the Yb-doped phosphosilicate fiber were setup. Thermal characteristics of the Yb-doped phosphosilicate fiber and the tunable fiber laser amplifier based on this fiber were found experimentally.

Experimental results show that the difference in the absorption and emission cross-sections triggered by change in temperature can significantly affect the overall laser and amplifier performance. With increasing temperature, the output power degradation of the amplifier based on Yb-doped phosphosilicate fiber was substantial, dropping nearly 20 % at 100 °C when the amplifier was wavelength tuned at 1060 nm. The trend of such change is likely to be greater in system working in a higher power where thermal condition is harsher and harder to control.

Understanding these characteristics is essential in modeling a fiber laser and an amplifier. Accounting for the thermal dependence of different

aspects analyzed here should substantially improve the accuracy of numerical models on Yb-doped phosphosilicate fiber lasers.

## Bibliography

- [1] R. J. Mears, L. Reekie, M. Jauncey, and D. N. Payne, “Low-noise erbium-doped fiber amplifier operating at 1.54  $\mu\text{m}$ ”, *Electron. Lett.* 26, 1026 (1987).
- [2] R. Paschotta et al., "Ytterbium-doped fiber amplifiers", *IEEE J. Quantum Electron.* 33 (7), 1049 (1997)
- [3] Y. Jeong et al., “Ytterbium-doped large-core fiber laser with 1.36 kW continuous-wave output power”, *Opt. Express* 12 (25), 6088 (2004).
- [4] D. J. Richardson, J. Nilsson, and W. A. Clarkson, “High power fiber lasers: current status and future perspective”, *J. Opt. Soc. Am. B* 27 (11), B63 (2010).
- [5] M. J. F. Digonnet, *Rare-Earth-Doped Fiber Lasers and Amplifiers*, 2nd edn., CRC Press, Boca Raton, FL (2001).
- [6] S. Suzuki, H. McKay, X. Peng, L. Fu, and L. Dong, “Highly ytterbium-doped phosphosilicate fibers for fiber lasers and amplifiers with high peak power,” *Proc. of CLEO/IQEC 2009*, Baltimore (USA), June 2009.
- [7] J. J. Koponen et al., “Measuring photodarkening from single-mode ytterbium doped silica fibers”, *Opt. Express* 14 (24), 11539 (2006).
- [8] M. Engholm and L. Norim, “Preventing photodarkening in ytterbium-doped high power fiber lasers; correlation to the UV-transparency of the core glass”, *Opt. Express* 16 (2), 1260 (2008).
- [9] M. Engholm and L. Norim, “Materials Optimization for Ytterbium-Doped High Power Fiber Lasers,” *Proc. of CLEO/QELS 2008*, San Jose (USA), May 2008.
- [10] T. H. Maiman, “Stimulated optical radiation in ruby”, *Nature* 187, 493 (1960).
- [11] A. E. Siegman, *Lasers*, University Science Books, Mill Valley, CA (1986).
- [12] Saleh and M. Teich, *Fundamentals of Photonics*, 2nd edn., Wiley, Hoboken, NJ (2007).
- [13] E. Desurvire, *Erbium-doped Fiber Amplifiers*, Wiley, New York, NY (1994).

- [14] P. Lacovara et al., "Room-temperature diode-pumped Yb:YAG laser", *Opt. Lett.* 16 (14), 1089 (1991).
- [15] Takunori Taira, William M. Tulloch, and Robert L. Byer, "Modeling of quasi-three-level lasers and operation of cw Yb:YAG lasers," *Appl. Opt.* 36 (9), 1867-1874 (1997).
- [16] A. J. Kenyon, "Recent developments in rare-earth doped materials for optoelectronics", *Prog. Quantum Electron.* 26, 225 (2002)
- [17] T.Y.Fan "Heat generation in Nd:YAG and Yb:YAG," *IEEE Journal of Quantum Electronics* 29 (6), 1457–1459 (1993).
- [18] G. C. Valley, "Modeling cladding-pumped Er/Yb fiber amplifiers", *Opt. Fiber Technol.* 7, 21 (2001)
- [19] D. Kouznetsov and J. V. Moloney, "Efficiency of pump absorption in double-clad fiber amplifiers. II. Broken circular symmetry", *J. Opt. Soc. Am. B* 19 (6), 1259 (2002)
- [20] D. Kouznetsov and J. V. Moloney, "Efficiency of pump absorption in double-clad fiber amplifiers. III: Calculation of modes", *J. Opt. Soc. Am. B* 19 (6), 1304 (2003)
- [21] R. Hui and M O'Sullivan, *Fiber Optic Measurement Techniques*, Academic Press, New York, NY (2008).
- [22] D. S. Sumida and T. Y. Fan, "Effect of radiation trapping on fluorescence lifetime and emission cross section measurements in solid-state laser media," *Opt. Lett.* 19, 1343-1345 (1994)
- [23] H. A. Haus, "The noise figure of optical amplifiers", *IEEE Photon. Technol. Lett.* 10 (11), 1602 (1998)
- [24] P. Weßels and C. Fallnich, "Noise figure measurements on Nd and Yb doped double-clad fiber amplifiers", *Opt. Express* 11 (13), 1531 (2003).

## 초 록

희토류가 도핑된 광섬유들 중 이터븀 광섬유는 비선형 및 열 통제가 중요한 고출력 영역 에서 매우 우수한 성능을 발휘한다. 광섬유 레이저와 증폭기를 이용하여 높은 출력을 얻기 위해서는 높은 수준의 희토류 도핑이 필요하다. 그러나 제한된 코어 사이즈와 광섬유 길이에서의 높은 레벨의 도핑은 클러스터링, 라이프타임의 감소, 그리고 포토다크닝을 유발한다.

Phosphosilicate기반의 이터븀 광섬유는 aluminosilicate기반의 이터븀 광섬유에 비해 상대적으로 긴 라이프타임과 더 높은 포토다크닝 면역력을 갖는다. 또한 phosphate 광섬유보다 높은 내열성을 갖고있다. 때문에Phosphosilicate 이터븀 광섬유는 고출력 레이저와 증폭기를 위한 좋은 옵션이다. Aluminosilicate 기반 이터븀 광섬유의 온도 의존성에 대해서는 많은 연구가 있었지만, Phosphosilicate 이터븀 광섬유의 온도 의존성에 대한 연구는 지금까지 거의 이루어지지 않았다.

본 논문에서는 Phosphosilicate기반의 이터븀 광섬유의 흡수 및 방출단면과 라이프타임 각각의 온도 의존성을 연구하였다. 또한 파장 조절 가능한 클래딩 펌프 이터븀 광섬유 증폭기의 온도 변화가 증폭기 이득에 미치는 영향에 대해 연구하였다. 이러한 Phosphosilicate기반의 이터븀 광섬유 온도의존성에 대한 연구는 광섬유레이저와 증폭기 모델링의 정확도를 높여줄 것으로 기대된다.

**주요어:** Phosphosilicate 이터븀 광섬유, 광섬유 증폭기, 온도 의존성, 포토다크닝, 고출력.

**학 번:** 2010-23280